At the Edge of the Universe:
Latest Results from the Deepest Astronomical Surveys
ASP Conference Series, Vol. 380, 2007
José Afonso, Henry C. Ferguson, Bahram Mobasher, and Ray Norris, eds.

Insights into Galaxy Evolution from Mid-infrared Wavelengths

Ranga-Ram Chary

Spitzer Science Center, Caltech, Pasadena CA 91125

Abstract. In this paper, I have attempted to highlight key results from deep extragalactic surveys at mid-infrared wavelengths. I discuss advances in our understanding of dust enshrouded star-formation and AGN activity at $0 < z < 3$ from *IRAS*, *ISO* and *Spitzer*. The data seem to indicate that about 70% of the co-moving star-formation rate density at $0.5 < z < 3$ is obscured by dust and that AGN, including obscured sources, account for <20% of the co-moving bolometric luminosity density. There is tentative evidence that the mode of star-formation changes as a function of redshift; star-formation at $z \sim 2$ is preferentially in massive, ultraluminous infrared galaxies (ULIRGs) while $z \sim 1$ sources are luminous infrared galaxies (LIRGs) which are about 1 mag fainter than ULIRGs in the near-infrared. This evolution of the star-formation mode, is similar to the evolution of the redshift distribution of X-ray sources as a function of X-ray luminosity and would suggest an extension of the downsizing hypothesis to include both AGN and star-forming galaxies. Measuring dust-enshrouded star-formation at $z > 3$ will become possible only with future facilities like ALMA. Currently, the presence of dust can only be assessed in a small fraction of the youngest starbursts at $z > 5$ by looking for redshifted large equivalent width Hα emission in broadband filters like the IRAC 4.5μm passband. Hα to UV ratios in these objects are a tracer of dust extinction and measuring this ratio in GOODS galaxies indicate dust in $\sim$20% of star-forming galaxies at $z > 5$. Finally, implications for reionization based on the measured stellar mass density and star-formation rates of galaxies at these redshifts are discussed.

1. Pros and Cons of the Mid-infrared

The mid-infrared regime of the electromagnetic spectrum, is generally defined by the wavelength range which can be detected with arsenic/antimony doped silicon semiconductors and spans 5$-$40μm. Extragalactic surveys in the mid-infrared are typically limited by background noise since the thermal emission from zodiacal light in the solar system peaks between 10$-$20μm (Kelsall et al. 1998). These wavelengths correspond to the trough between the optical/near-infrared and far-infrared wavelengths in the spectrum of the extragalactic background light (EBL). To illustrate, the EBL intensity derived by integrating the light from galaxies detected at 15 and 24 μm is around 2.5-5 nW m^{-2} sr^{-1} while the EBL intensity at both 140 μm and 2.2 μm has a value of about $\sim$25 nW m^{-2} sr^{-1} (Lagache et al. 2005). Since the EBL is the sum total of redshifted emission from sources integrated over the observable Universe, the bulk of which arises from galaxies at $z < 1.5$, this implies that the energy emitted at near- and far-infrared wavelengths is almost an order of magnitude larger than that at mid-infrared wavelengths. This is generally true even for individual star-forming galaxies; the

mid-infrared regime lies between the optical/near-infrared stellar photospheric emission and the far-infrared emission from dust heated to T∼20-40K, both of which together dominate the bolometric luminosity of the galaxy.

The mid-infrared is a complicated spectral region representing the integrated emission from broad polycyclic aromatic hydrocarbon features, continuum emission from dust grains between 300K and 40K and silicate absorption (Desert et al. 1990). As a result, even small errors in redshifts translate into large errors in spectral $k-$ corrections making estimates of the true rest-frame luminosity difficult (Figure 1).

Despite these difficulties, the mid-infrared is the most powerful tracer of dust enshrouded star-formation activity out to redshifts of 3 (Figure 2). This is possible because of the tight correlation between mid- and far-infrared emission on both sub-galactic and galactic scales (Calzetti et al. 2005; Chary & Elbaz 2001). For example, rest-frame 7μm emission has been shown to trace L_{IR} with a 1σ scatter of 40% in the local Universe. The correlation appears to hold even in the $z \sim 1$ Universe as determined from a comparison between 7μm, 70μm and 1.4 GHz radio luminosities of individual galaxies. However, there is some evidence that at low metallicities ($Z < 1/4\ Z_{\odot}$) the PAH line strengths show significant differences (Smith et al. 2007). On the instrumentation side, mid-infrared observations have arcsec sized beams even with small ∼1m class telescopes. This has the benefit of alleviating the effects of source confusion. It also simplifies the identification of the counterparts of mid-infrared sources at optical/near-infrared wavelengths and thereby enables the measurement of their spectroscopic redshifts. Finally, mid-infrared arrays suffer less from latents and transient effects in their responsivity than far-infrared arrays and need to be cooled only down to a few degrees Kelvin instead of the milli-kelvin requirements of submillimeter bolometers.

2. Key Extragalactic Mid-infrared Surveys

Deep *IRAS* 12 μm and 60 μm observations in the direction of the North Ecliptic Pole (Hacking & Houck 1987), were the first to provide evidence for redshift evolution of the infrared luminosity function of galaxies. The survey measured a source density of ∼30 deg^{-2} down to 10 mJy which was a factor of 1000 deeper than the *IRAS* All Sky Survey. The source counts down to this flux density limit provided tentative evidence for evolution of the infrared luminosity function to redshifts of 0.2 (Hacking et al. 1987).

Subsequent mid-infrared surveys which have revolutionized our understanding of galaxy evolution at cosmological distances are those undertaken with *ISOCAM* at 15 μm surveys (Genzel & Cesarsky 2000) and *Spitzer*/MIPS at 24μm.

ISOCAM undertook a variety of deep 15 μm surveys, the deepest of which, apart from those in lensing cluster fields, was in the Hubble Deep Field North (Aussel et al. 1999). These observations which covered an area of ∼ 20 arcmin^2 centered on the HDF-N, were sensitive down to a flux limit of 100 μJy and reliably detected about ∼40 sources. The differential source counts was more than an order of magnitude larger than expected if the local infrared luminosity function of galaxies did not evolve with redshift. This data provided reliable evidence for a strong ∼ $(1+z)^4$ luminosity evolution of infrared luminous galaxies. Identi-

fication of the optical counterparts of the 15μm sources and measurement of their redshifts from ground-based spectroscopic surveys (Wirth et al. 2004; Cohen et al. 2000) revealed that these were galaxies at $z \sim 0.5 - 1.0$. Cross-correlation with X-ray surveys from Chandra and XMM (Brandt, these proceedings) as well as their optical spectra revealed that only about 20% of these objects appear to have AGN in them implying that star-formation was powering the bulk of the emission. As a result, one could apply the local correlation between mid- and far-infrared luminosities, which revealed that these were infrared luminous galaxies with L_{IR}=L(8$-$1000μm)$> 10^{11}$ $L_\odot$ with the majority of them being LIRGs (10^{11} $L_\odot < L_{IR} < 10^{12}$ $L_\odot$). The estimates of their star-formation rates are in the range of 10-100 $M_\odot$ yr^{-1}, most of which is dust obscured. For the subset of sources which are radio detected, the derived far-infrared luminosities of these sources agree well with the radio-FIR correlation in the local Universe providing evidence against an evolution of the far-infrared spectral energy distribution with redshift. The SED fitting also yielded a contribution of *ISOCAM* galaxies to the DIRBE observed far-infrared background of 65$\pm$30% (Elbaz et al. 2002). The contribution of dusty starbursts to the total EBL has since been confirmed more recently by stacking *Spitzer* far-infrared data on mid-infrared sources by Dole et al. (2006).

Phenomenological models which attempted to fit the source counts from surveys at various wavelengths, based on local galaxy templates, indicated a strong evolution of the far-infrared luminosity density with redshift (Chary & Elbaz 2001; Franceschini et al. 2001). These models revealed that the far-infrared luminosity density is between a factor of 5$-$10 higher than the UV luminosity density at $z \sim 1$ implying an increase in the average dust extinction in the Universe from E(B-V)$\sim$0.15 at $z \sim 1$ to E(B-V)$\sim$0.3 at $z \sim 1$. However, it is difficult to have these models account for cosmic variance which cause source counts to vary by as much as a factor of 2 between different fields. Also, phenomenological models are degenerate in factoring in the amount of luminosity evolution and density evolution in the infrared luminosity function due to the difficulty in measuring the faint end slope of the luminosity function. Various models which simultaneously fit the source counts at different wavelengths have slightly different parameters for the redshift evolution of LIRGs and ULIRGs (Chary & Elbaz 2001; Lagache et al. 2004). In addition, the underlying mid and far-infrared templates used in the models strongly affect the evolution parameters. Nevertheless, the evolution of the far-infrared luminosity density appears to be robust to these parameters.

There were two significant problems. Due to the fact that the PAH features get redshifted out of the *ISOCAM* 15μm bandpass at $z \sim 1.2$, it was impossible to assess evidence for evolution of the infrared luminosity function at higher redshift without using galaxy counts at 850μm which are discussed elsewhere (R. Ivison, these proceedings). Secondly, the integral of the co-moving star-formation rate density from the models overpredicted the measured comoving stellar mass density seen by Dickinson et al. (2003). This could either be due to the stellar mass density being underestimated from the uncertain contribution of the high Mass/Light ratio old stellar component in galaxies. Alternately, it could be due to the fact that at high redshifts, the mid-infrared determined bolometric luminosity densities are overestimates. Deep, wide *Spitzer* surveys

(e.g. Dickinson et al. *Spitzer* GO-3) are well positioned to address this problem by providing 70μm coverage of large numbers of $z > 2$ galaxies, enabling bolometric luminosities to be validated using stacking analysis.

3. GOODS MIPS 24 μm Survey

The Great Observatories Origins Deep Survey 24μm observations were taken with the Multiband Imaging Photometer Spectrometer (MIPS; Rieke et al. (2004)). The 24μm passband can detect PAH emission out to $z \sim 3$. However, unless the observations are adequately deep, observations would be unable to detect typical infrared luminous galaxies much beyond the limits set by *ISOCAM*. For example, at a flux limit of 80μJy, 24 micron observations are sensitive to a typical $3{\times}10^{11}$ $L_{\odot}$ out to $z \sim 1.2$ which is about the same as what the *ISOCAM* HDF observations could detect such objects out to. By going down to 20μJy, such galaxies are now being detected out to redshifts 2.5, enabling a comparison with the $z \sim 2$ submillimeter galaxy population and $z \sim 3$ Lyman-break galaxy population.

The *Spitzer* beam size at 24μm is 5.7$''$ FWHM which raises the issue of source confusion. However, due to the accurate pointing of *Spitzer* and $\sim$0.2$''$ rms with which we can align the 24μm images with observations at 3$-$8μm, the concerns of confusion noise placing a floor on the sensitivity are misplaced. The surface density of sources is 17 arcmin^{-2} in GOODS-N and 24 arcmin^{-2} in GOODS-S. Also, at this resolution, the vast majority of extragalactic sources are point sources. Using a prior position based point source fitting algorithm, we have been able to extract sources with a completeness of 84% at 24μJy (Figure 3). The 5σ point source sensitivity limit of this survey is 25μJy. The fundamental reason for the success of this technique is because every MIPS source is detected in deep 3.6μm observations.

The differential 24μm source counts are similar in shape to the 15μm counts with a break in dN/dS at 400μJy (Figure 3). The slope of the counts at fainter fluxes is $\sim S^{-1.6}$. One of the most salient features of the 24μm counts is they peak (in dN/dS$\times S^{2.5}$) at fainter flux values than predicted from the phenomenological models which are fit to the multiwavelength counts. Attempts to resolve this have included changing the evolution of the LIRG to ULIRG ratio with redshift as in Chary et al. (2004) or weakening the strength of the 11 and 12μm PAH (Lagache et al. 2004) in the galaxy templates so that objects which contribute to the peak of the 15μm counts contribute at fainter fluxes to the 24μm counts.

There is little observational evidence for a weakening of the 11 and 12μm PAH (e.g. Pope et al. 2006, these proceedings). Stacking of IRS spectra of 24μm sources indicate that apart from an underlying hot dust continuum which might lower the equivalent widths of all PAH between 6 and 12μm, the relative line ratios do not vary except for metal poor galaxies. Since dusty starbursts appear to be in massive galaxies, which have also enriched the ISM in the process of increasing the dust content, there is less concern that the bolometric luminosities for the bulk of the galaxies are incorrect although some recalibration of the libraries probably have to be done for the SEDs of the most luminous galaxies ($L_{IR} > 10^{13}$ $L_{\odot}$) for which no low-redshift counterparts exist.

4. Evidence for "Downsizing" in AGN and Galaxies

From the redshifts and 24μm flux densities of individual sources, we can calculate their far-infrared luminosity using the template fitting approach (Chary & Elbaz 2001). The accuracy of this approach has been verified at $z < 2$ from 70μm and 850μm stacking of LIRGs and ULIRGs. Also, the spectral energy distribution of galaxies at $z \sim 2$ selected using the BzK technique also appear to match the templates spectral energy distribution closely (Daddi et al. 2005). The far-infrared luminosity can be converted into a star-formation rate using the conversion factor in Kennicutt et al. (1998). One possible uncertainty in this conversion is estimating the contribution to the far-infrared luminosity from dust being heated by the evolved stellar population. Deep optical surveys provide a measure of the star-formation seen in the rest-frame ultraviolet. Since the bulk of the far-infrared emission is dust heated by the ultraviolet radiation field which is dominated by star-formation, adding the UV and FIR star-formation rates yields the star-formation rates of individual objects.

Although the stellar masses of galaxies can be derived using SED fits to the multiband photometry, a comparison between the 3.6μm magnitudes of LIRGs and ULIRGs which traces rest-frame near-infrared emission provides a good estimate of the stellar mass. The photometry indicates that LIRGs at $z \sim 1.5$ have a median 3.6μm brightness of 21.2 AB mag while ULIRGs are 20.5 AB mag. At $z \sim 2.4$, LIRGs are 22.5 AB mag while ULIRGs are 21.5 AB mag. Thus ULIRGs are systematically, about 1 AB mag brighter at 3.6μm indicating that they are more massive.

Finally, AGN can be estimated in the $0.5 < z < 3$ range by identifying power laws from hot dust in the observed 5.8$-$24μm range. Alternately, the X-ray luminosity and photon index of sources provides a good measure of AGN activity. We caution that Compton-thick AGN are undetected even in the deepest Chandra surveys beyond $z \sim 0.6$ and the IRAC power law identification of AGN breaks down at redshifts of $z > 2$ because dust sublimes at around $\sim$1500$-$2000 K corresponding to rest-frame $\sim$2μm. At $z \sim 2$, the 2μm emitting hot dust is redshifted out of the 5.8μm bandpass.

Putting these various datasets together, we confirm the *ISOCAM* result implying an evolution of the far-infrared luminosity density with redshift (Babbedge et al. 2006; Le Floc'h et al. 2005; Perez-Gonzalez et al. 2005). However, the data also indicate an evolution of the galaxies dominating the co-moving star-formation rate density. At $z \sim 1$, LIRGs which typically have stellar masses of $\sim 10^{9-10}$ $M_\odot$ and star-formation rates of 10-100 $M_\odot$ yr^{-1} are dominating the energetics. At $z \sim 2$, it is the ULIRGs which have stellar masses $>10^{10}$ $M_\odot$ that are dominating the star-formation rate density (Figure 4). The AGN contribution to the luminosity density at both redshifts appear to less than $\sim$20%. Thus, lower mass galaxies form later in cosmic time and more massive galaxies build their stellar mass earlier.

This trend is similar to the redshift distribution of X-ray sources as a function of X-ray luminosity (Ueda et al. 2003). The X-ray data seem to suggest that the most massive ($\sim 10^9$ $M_\odot$) nuclear black holes built up their mass in a luminous accretion event around $z \sim 2-3$ while the ULIRGs were building up their stellar mass. The lower mass black holes on the other hand, grew around $z \sim 1$ when the LIRGs were building up their stellar mass providing impetus

for the downsizing scenario extending to AGN and starbursts. Since low mass galaxies are more numerous and populate the Hubble sequence, this implies that the Hubble sequence was probably in place only at $z < 1$.

However, there are potential systematics. There is some evidence in our IRS spectra that the color temperatures of the mid-infrared spectra are relatively cool. Templates of local galaxies which are used to derive the bolometric corrections typically have steeply rising hot dust continuum with increasing L_{IR}. This would imply that bolometric corrections might have been overestimated and many of the objects are less luminous. The effect is particularly important in the $2 < z < 3$ regime where we have limited checks on the shape of the template from stacking analysis. There is also evidence in some objects that continuum from an AGN results in the 6.2μm PAH equivalent width being reduced by a factor of 3 compared to local starburst galaxies such as M82. This would again imply an incorrect bolometric correction in the $z > 2$ sources. Finally, due to the difficulty in identifying AGN at $z > 2$ from the IRAC colors, we might be underestimating the AGN contribution which would be predominantly to the brightest 24μm sources thereby lowering the ULIRG contribution. Further checks, especially in the $2 < z < 3$ range, where both photometric and spectroscopic redshifts are limited are essential to verify the result shown in Figure 4.

5. Dust at Higher Redshifts and Implications for Reionization

Detecting dust emission at redshifts greater than 3 is difficult. The strongest PAH features at 6.2 and 7.7 μm are redshifted out of the MIPS 24μm bandpass. Only sources with large AGN contributions displaying significant hot dust emission are detected at $z > 3$ at 24μm. It appears that the equivalent width of the 3.3μm PAH is low enough that it would be undetectable above the stellar continuum and the correlation between 3.3μm emission and L_{IR} is not well established. 70μm surveys are about one to two orders of magnitude less sensitive than required to detect dust in all but the most hyperluminous sources. As a result, at $z > 3$, 850μm surveys are best suited for detecting dust emission but the current sensitivity limits (Figure 2) will not be significantly improved until the Atacama Large Millimeter Array (ALMA) becomes operational.

One possible technique has been to measure redshifted Hα emission through broadband photometry. This technique can only be applied over a limited redshift range. In Chary, Stern, & Eisenhardt (2005), we demonstrated the possibility that the enhanced 4.5μm/3.6μm flux ratio of the lensed $z = 6.56$ galaxy HCM6A is due to large equivalent width Hα. A study of the broadband photometry in GOODS galaxies has since revealed that about 10$-$20% of spectroscopically confirmed $z > 5$ objects show a similar enhancement in the 4.5μm flux (Figure 5; Chary et al. 2007). The Hα determined star-formation rates are on average higher by a factor of $\sim$3, compared to the UV determined star-formation rate, indicating the presence of dust in a small fraction of high redshift objects. The presence of dust within 1 Gyr of the Big Bang argues for the production of dust from SNe since red giants and AGB stars have had insufficient time to evolve.

Since the dust content correlates with the number of SNe, it must increase with decreasing redshift and is presumably directly correlated to the increase

in stellar mass. This implies that for a small fraction of objects, the measured star-formation rate from the UV continuum is lower than the true star-formation rate. Since typical starbursts have an e-folding time associated with them, the conclusion is that that the star-formation rate ($\dot{\rho}_*(t)$) of a galaxy at some time $t < t'$ in its past history must be:

$$\dot{\rho}_*(t) = \dot{\rho}_*(t') \exp[-(t - t')/\tau_{SFR}] \exp[-\tau(t) + \tau(t')] \quad (1)$$

where,

$$\tau(t') \propto \int_0^{t'} \dot{\rho}_*(t) dt \quad (2)$$

τ_{SFR} is the e-folding time for the star-burst while $\tau(t)$ is the extinction in the star-formation rate metric (i.e. UV wavelengths) at time t. Naturally, $\tau(t) < \tau(t')$.

We have now been able to measure the star-formation rate and stellar mass density in galaxies at $z \sim 6$. For canonical estimates of the escape fraction (fesc$\sim$0.15) and clumping factor (C=30), the measured star-formation rate at $z > 6$ falls more than a factor of 10 short of the minimum needed to reionize the IGM. However, if the dust content is increasing with redshift, the past star-formation rate must be higher not just by the e-folding time of the burst but also by the increase in dust extinction which is directly proportional to the stellar mass.

The past history of star-formation can either be identified by fitting SEDs to the multiband photometry and extrapolating backwards in time or by fitting an evolving starburst model to the measured star-formation rate and stellar mass density at $z \sim 6$ (Figure 6). From rest-frame ultraviolet observations of Lyman-break galaxy samples (Bouwens et al. 2006), it appears that the star-formation rate density is decreasing at $z > 6$, while from the extrapolation process the star-formation rate density must be increasing at higher redshifts to reproduce the observed stellar mass density. This discrepancy is probably attributable to the large completeness corrections associated with identifying galaxies at $z > 7$ using current instrumentation.

The primary conclusions are as follows: 1) If the measured star-formation rate density and stellar mass density at $z \sim 6$ are accurate (Yan et al. 2006; Chary et al. 2007; Eyles et al. 2005; Stark et al. 2007), then reionization must be a brief, inhomogeneous processing lasting only 20-50 Myr at $6 < z < 7$; 2) If the process of reionization starts at $z \sim 9$ and is prolonged, then the stars that dominate the reionization process must not contribute to the stellar mass density at $z \sim 6$ i.e. the mass of stars and remnants at $z \sim 6$ must be higher than the measured stellar mass by a factor of $\sim$10. This would suggest a contribution from high mass, zero metallicity Population III stars or from the low mass end of the galaxy mass function. Either of these scenarios are unnecessary if the escape fraction and clumping factor are significantly different from the canonical estimates of 0.15 and 30 respectively.

Acknowledgments. I wish to thank the organizers for a very productive and enjoyable meeting. I would like to acknowledge contributions from various members of the GOODS team which resulted in the material presented in this paper. This work is partly funded by NASA through Contract Number 1224666 issued by JPL/Caltech under NASA contract 1407.

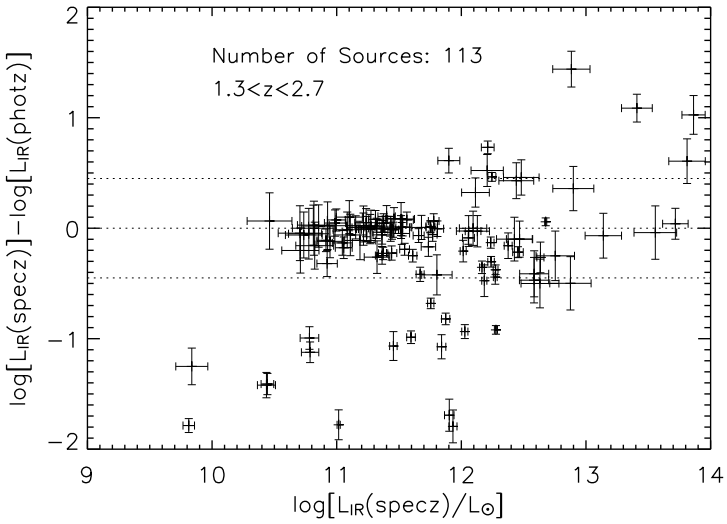

Figure 1. Uncertainty in determining L_{IR} from monochromatic observed 24μm fluxes due to an error in the photometric redshift estimate. Due to the interplay of emission and absorption features in the mid-infrared, small errors in redshift estimates result in the incorrect far-infrared template being chosen from template libraries. This manifests itself into large errors in the bolometric correction and thereby the derived bolometric luminosity of objects. The 1σ scatter in the derived L_{IR} due to typical optical/near-infrared photometric redshifts is a factor of 3 for a 1σ scatter in Δz of 0.24 which corresponds to a $\sigma(\Delta z)/(1+z_{spec})\sim$0.1.

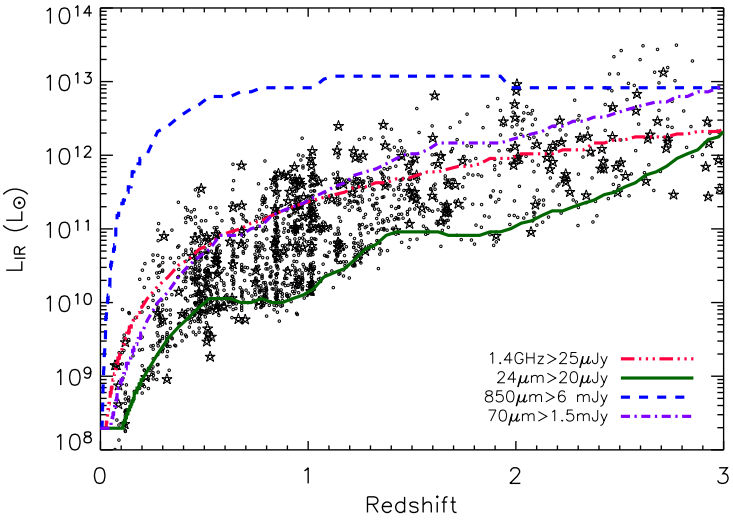

Figure 2. Sensitivity of deep surveys at different wavelengths to L_{IR}=L(8−1000 μm), a proxy for star-formation rate. Also plotted are sources with either photometric or spectroscopic redshifts. Stars indicate X-ray sources i.e. AGN, while circles are star-forming galaxies. The GOODS 24 μm observations are at least an order of magnitude more sensitive to dust obscured star-formation and AGN activity than other surveys.

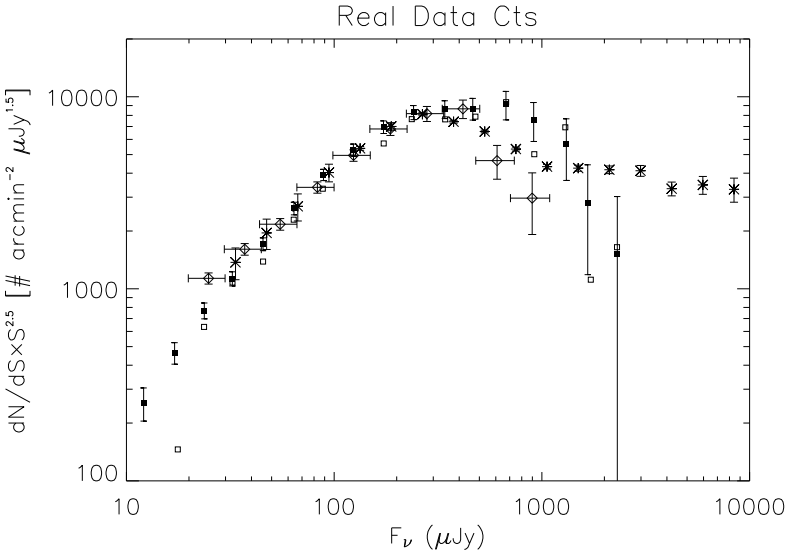

Figure 3. Differential extragalactic source counts at 24μm in the GOODS-N field. The empty squares are the measured counts, the solid squares are the counts corrected for completeness, the open diamonds are the completeness corrected counts in the GOODS test field in ELAIS-N1 (Chary et al. 2004), while the asterisks are the counts in various other fields (Papovich et al. 2004; Marleau et al. 2004). Application of the prior-based deblending technique results in an extracted source catalog which is 84% complete at 24μJy illustrating that source confusion is not a significant source of noise in GOODS.

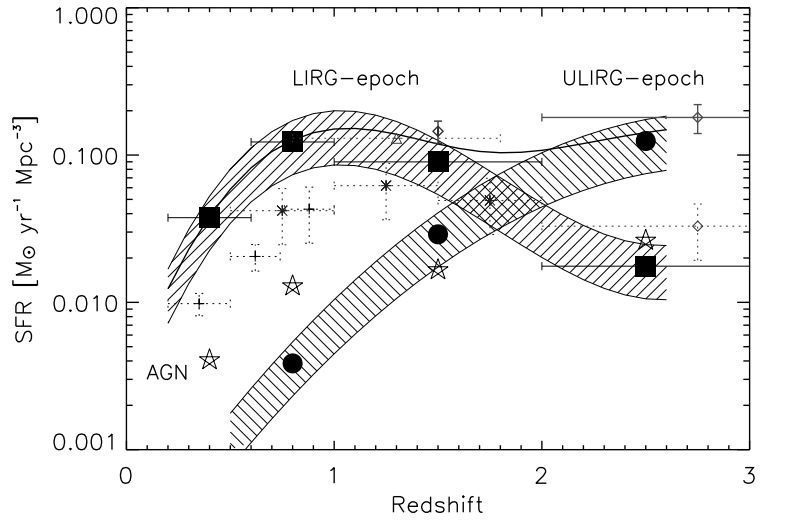

Figure 4. Relative contribution of LIRGs (hatched region), ULIRGs (back-hatched region) and AGN (stars) to the co-moving far-infrared luminosity density between $0 < z < 3$. The dotted symbols underlying are various measures of star-formation from the UV and Hα referenced in Chary & Elbaz (2001). The systematic uncertainty in this measurement is a factor of $3-4$ at $z > 2$ due to the limited number of sources with spectroscopic redshifts and uncertainty in the AGN contribution (see text).

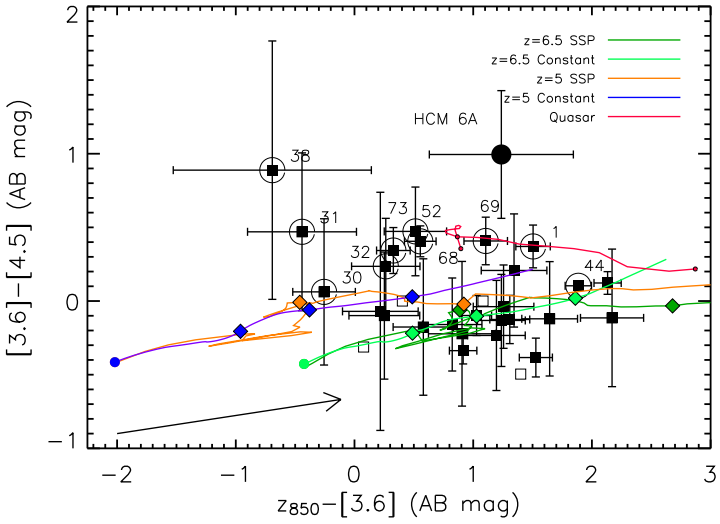

Figure 5. Identification of Hα in emission using broadband colors. Circled sources are candidate Hα emitters with $z_{spec} > 5$ (Chary et al. 2007, 2005). Comparison of the Hα SFR to the UV continuum derived star-formation rate provides a unique technique to measure dust obscured star-formation at $z > 5$. However, this technique can be used only in the most violently star-forming galaxies because the equivalent width of Hα must be very high for it to be detectable in a broadband filter like *Spitzer*/IRAC 4.5μm.

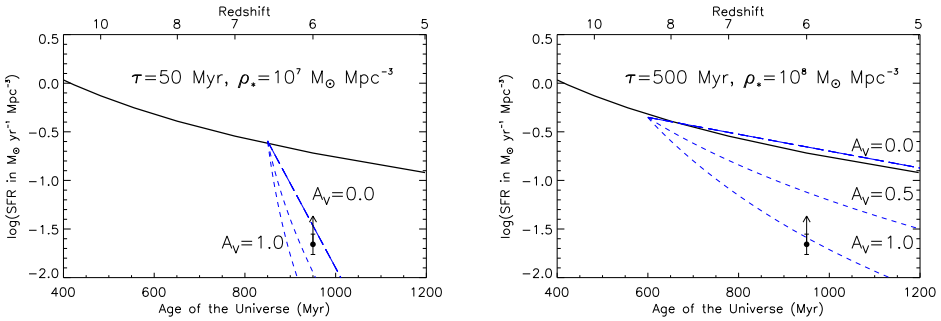

Figure 6. *Left Panel*: The solid black line shows the minimum star-formation rate as a function of redshift, for a Salpeter IMF, which is required to reionize the IGM (escape fraction of 0.15 and clumping factor of 30). The black symbol shows the measured star-formation rate density at $z\sim6$ (Bouwens et al. 2006). The long-dashed line, shows the star-formation history of the Universe required to reproduce the measured stellar mass density as well as the star-formation rate density at $z\sim6$. Since the long dashed line can exceed the solid line for a brief interval of time, reionization must be a brief process lasting 20-50 Myr at $z\sim6.5$. *Right Panel*: If on the other hand reionization took place at $z\sim9$, then either the stellar mass density at redshift 6 must be $\times10$ higher than what is measured due to a steep faint end mass function or the sources responsible for reionization at $z\sim9$ do not contribute to the stellar mass density at $z\sim6$. The short dashed lines show the role of increasing extinction on the measured star-formation rate density for A_V=0.5 mag and A_V of 1 mag.

References

Aussel, H. et al. 1999, A&A, 342, 313
Babbedge, T. S. R. et al. 2006, MNRAS, 370, 1159
Bouwens, R. J., Illingworth, G. D., Blakeslee, J. P., & Franx, M., 2006, ApJ, 653, 53
Calzetti, D., et al., 2005, ApJ, 633, 871
Chary, R., Elbaz, D., 2001, ApJ, 556, 562
Chary, R., et al., 2004, ApJS, 154, 80
Chary, R.-R., Stern, D., & Eisenhardt, P. 2005, ApJ, 635, L5
Chary, R., et al., 2007, ApJ, submitted
Cohen, J., et al., 2000, ApJ, 538, 29
Daddi, E., et al., 2005, ApJ, 631, L13
Desert, F.-X., et al., 1990, A&A, 237, 215
Dickinson, M., et al., 2003, ApJ, 587, 25
Dole, H., et al., 2006, A&A, 451, 417
Elbaz, D., et al., 2002, A&A, 384, 848
Eyles, L., Bunker, A., Stanway, E., Lacy, M., Ellis, R., & Doherty, M. 2005, MNRAS, 364, 443
Fazio, G., et al., 2004, ApJS, 154, 10
Franceschini, A., et al., 2001, A&A, 378, 1
Genzel, R., & Cesarsky, C., 2000, ARA&A, 38, 761
Hacking, P., & Houck, J. R., 1987, ApJ, 63, 311
Hacking, P., et al., 1987, ApJ, 316, L15
Kelsall, T., et al., 1998, ApJ, 508, 44
Kennicutt, R., 1998, ARA&A, 36, 189
Lagache, G., 2004, ApJ, 154, 112
Lagache, G., 2005, ARA&A, 43, 727
Le Floc'h, E., 2005, ApJ, 632, 169
Marleau, F., et al., 2004, ApJS, 154, 66
Pope, A., et al., 2007, these proceedings
Perez-Gonzalez, P., 2005, ApJ, 630, 82
Rieke, G., et al., 2004, ApJS, 154, 25
Papovich, C., et al., 2004, ApJS, 154, 70
Smith, J. D. T., et al. 2007, ApJ, 656, 770
Stark, D. P., Bunker, A. J., Ellis, R. S., Eyles, L. P., & Lacy, M. 2007, ApJ, 659, 84
Ueda, Y., et al., 2003, ApJ, 598, 866
Wirth, G., et al., 2004, AJ, 127, 3121
Yan, H., et al., 2006, ApJ, 651, 24